Korean J. Chem. Eng., 33(6), 1889-1896 (2016)
DOI: 10.1007/s11814-016-0027-4

pISSN: 0256-1115
eISSN: 1975-7220

Optimization study of a batch chromatographic process based on Amberchrom-CG161C adsorbent for separation of valine from a ternary amino acid mixture

Sungyong Mun†

Department of Chemical Engineering, Hanyang University, Seoul 04763, Korea
(*Received 16 October 2015 • accepted 25 January 2016*)

Abstract−The optimal design of the batch chromatographic process for separation of valine (product) from isoleucine and leucine (side-products) was carried out by using the relevant optimization tool that was prepared on the basis of an up-to-date genetic algorithm. In such an optimal design, the flow rate, feed size (Δ_{feed}), eluent gap size (Δ_{gap}), and product collection time were optimized to maximize the valine productivity of the batch chromatographic process under consideration. The results showed that the valine productivity was governed by the flow rate in the region of low flow rates, whereas it was governed by the $\Delta_{gap}/\Delta_{feed}$ factor in the region of high flow rates. Finally, the effect of valine yield on the productivity was investigated, followed by providing the proper operating conditions that could be advantageous to both valine productivity and valine yield.

Keywords: Valine Separation, Batch Chromatographic Process, Process Optimization

INTRODUCTION

Valine has been credited as one of the highly profitable amino acids, and its useful applicability has been confirmed in various industries [1-4]. The recent way for valine production is to utilize a biotechnological route based on *Corynebacterium* bacteria fermentation [1-4]. One of important issues in such valine production is to separate valine (target product) from isoleucine and leucine (side-products) [5]. To deal with this issue, we developed a customized batch-chromatographic process for separation of valine from isoleucine and leucine. There are two main points to be considered for such a separation process development. First, a reliable adsorbent with large particle size and high selectivity should be employed. Secondly, the separation process to be developed should be well optimized to guarantee high purity and high productivity.

In regard to the first point, it is worth referring to the latest literature information [5,6], in which an Amberchrom-CG161C resin was reported to be effective in valine separation. On the basis of such information, we selected an Amberchrom-CG161C resin as the adsorbent for the batch chromatographic process for valine separation. To address the second point, the optimization of the batch chromatographic process based on the Amberchrom-CG161C adsorbent was carried out in such a way that its valine productivity could be maximized under a given purity requirement for valine separation from isoleucine and leucine. To facilitate this work, a highly efficient electronic tool for the optimization of a batch chromatographic process was prepared on the basis of non-dominated sorting genetic algorithm with elitism and jumping genes (NSGA-II-JG) [7,8], which is characterized by the jumping gene operation that is known to be effective in preventing a local optimum and increasing convergence speed. The optimization results were analyzed in a systematic way, and used to clarify which factors have a dominant effect on the productivity of the customized batch-chromatographic process for valine separation. Furthermore, the effect of a target level of valine yield on the optimized valine productivity was investigated. Finally, the batch chromatographic process that can be advantageous to both valine productivity and valine yield was proposed.

THEORY

1. Mathematical Model for the Simulation of a Chromatographic Separation Process

The migration behavior of solutes in a chromatographic separation process is usually governed by several mass-transfer mechanisms such as convection, axial dispersion, film mass-transfer, and intra-particle diffusion. To describe such dynamic behaviors of solutes, several chromatographic models have been developed in the literature [9-13]. The usefulness of such models is particularly pronounced in the stage of optimizing a chromatographic process, because they can be combined with a well-established optimization algorithm in order to prepare a highly efficient optimization tool for a target process.

In this study, a lumped mass-transfer model, which has been one of well-established rate-models in the literature [10-13], was employed as a major frame of simulation for the batch chromatographic process of our interest. Its effectiveness in predicting the migration behavior of solutes and optimizing a variety of chromatographic processes has been verified in many previous studies [10-13]. This model consists of differential mass balance equations for the mobile and pore phases, which are presented below [10,11].

†To whom correspondence should be addressed.
E-mail: munsy@hanyang.ac.kr
‡This article is dedicated to Prof. Huen Lee on the occasion of his retirement from KAIST.

$$\varepsilon_b \frac{\partial C_{b,i}}{\partial t} + (1-\varepsilon_b) K_{f,i}(C_{b,i} - C_i^*) + u_0 \varepsilon_b \frac{\partial C_{b,i}}{\partial z} - \varepsilon_b E_{b,i} \frac{\partial^2 C_{b,i}}{\partial z^2} = 0 \quad (1a)$$

$$\varepsilon_p \frac{\partial C_i^*}{\partial t} + (1-\varepsilon_p) \frac{\partial q_i}{\partial t} = K_{f,i}(C_{b,i} - C_i^*) \quad (1b)$$

where the subscript i stands for different solutes; $C_{b,i}$ is the mobile-phase concentration; C_i^* is the average pore-phase concentration; q_i is the solid-phase concentration, which is in equilibrium with C_i^*; ε_b is the bed voidage; u_0 is the liquid interstitial velocity; ε_p is the particle porosity; and E_b is the axial dispersion coefficient. In addition, K_f is the lumped mass-transfer coefficient, which can be estimated from the following equation [10,11].

$$\frac{1}{K_f} = \frac{(d_p/2)^2}{15\varepsilon_p D_p} + \frac{(d_p/2)}{3k_f} \quad (2a)$$

where d_p is the diameter of adsorbent particle; D_p is the intra-particle diffusivity; and k_f is the film mass-transfer coefficient. The boundary conditions are presented below.

$$z=0, \quad \left.\frac{\partial C_{b,i}}{\partial z}\right|_{z=0} = \frac{u_0}{E_{b,i}}[C_{b,i}(t, z=0) - C_{in,i}(t, z=0)] \quad (2b)$$

$$z=L_c, \quad \left.\frac{\partial C_{b,i}}{\partial z}\right|_{z=L_c} = 0 \quad (2c)$$

where $C_{in,i}$ is the inlet concentration of component i.

The equilibrium relationship between q_i and C_i^* in the above model equation is usually expressed by an adsorption isotherm, which is given below in the case of a linear adsorption relationship.

$$q_i = H_i C_i^* \quad (3)$$

where H_i is the Henry constant of component i.

To solve the aforementioned model equations, a biased upwind differencing scheme (BUDS) with 120 nodes per column and gear integration method were used. All of these numerical computations were on an Aspen Chromatography simulator.

2. Key Operating Parameters and Performance Criterion in a batch Chromatographic Separation Process

A batch chromatographic separation process is usually operated in such a way that the sequential steps of feed injection and eluent elution are repeated cyclically at the column inlet, while the other sequential steps of product collection and waste discard are

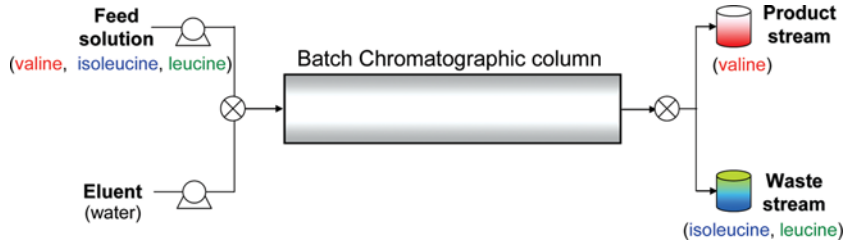

Fig. 1. Schematic diagram of the batch chromatographic process for separation of valine (product) from isoleucine and leucine (impurities).

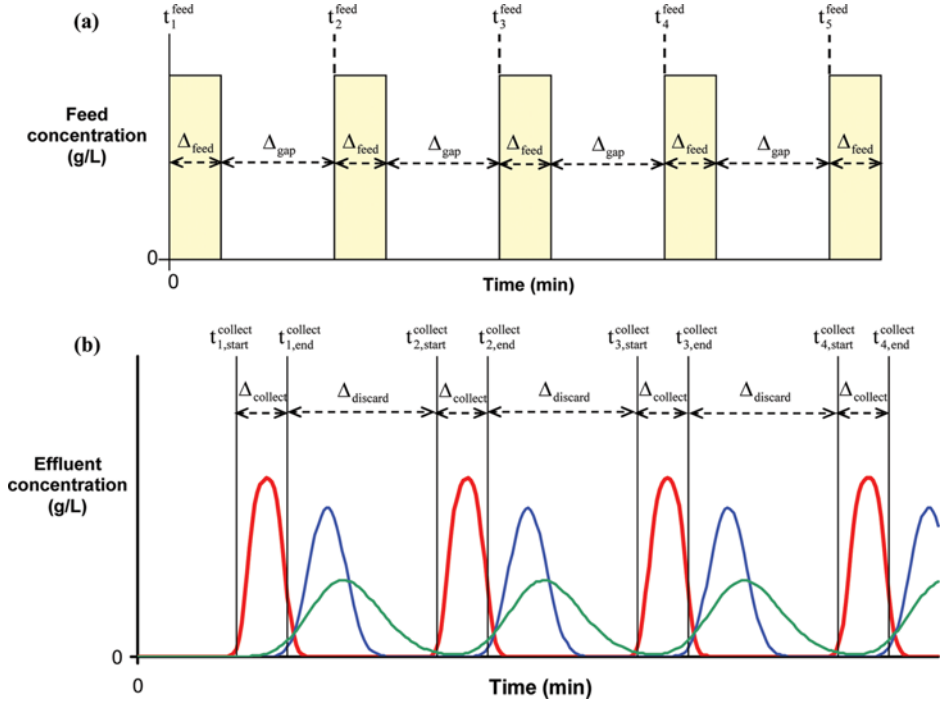

Fig. 2. Patterns of key operations in a batch chromatographic process. (a) Operations at the column inlet (feed injection and eluent elution), (b) operations at the column outlet (product collection and waste discard). : valine (product), : isoleucine, : leucine.

repeated cyclically at the column outlet [14]. The schematic diagram of such operation is illustrated in Fig. 1 for the case of separating valine from isoleucine and leucine, which is the targeted task in this work.

As seen in Fig. 1, two pumps are placed ahead of the feed loading position. One of the pumps is used to deliver a stream of feed solution, which is the mixture of the three amino acids dissolved in an eluent. The other pump is used to deliver an eluent during the gap time between the adjacent feed injections. In addition, two reservoirs are placed behind the column outlet. One of the reservoirs is used to collect a stream of the separated valine product while the other deals with a waste stream. Under such arrangements of pumps and reservoirs, the aforementioned cyclic operations are implemented.

The key parameters related to the operation of such a batch chromatographic process include flow rate, feed size, gap size, feed injection time, and product collection time. To explain the concepts of these parameters more clearly, several terms available in the literature [14] are introduced here. First, the time that the first feed injection begins is defined as t_1^{feed}, which is usually set to zero. The time that the n^{th} feed injection begins (t_n^{feed}) can thus be expressed as follows (Fig. 2(a)):

$$t_n^{feed}=(n-1)\cdot(\Delta_{feed}+\Delta_{gap}) \tag{4}$$

where Δ_{feed} and Δ_{gap} are the feed and gap sizes in time unit, respectively. In this situation, the starting time and the ending time of the n^{th} product collection (denoted as $t_{n,\,start}^{collect}$ and $t_{n,\,end}^{collect}$ respectively), which are illustrated in Fig. 2(b), can be related to Δ_{feed} and Δ_{gap} by the following equation [14].

$$t_{n,\,start}^{collect}=(n-1)\cdot(\Delta_{feed}+\Delta_{gap})+t_{1,\,start}^{collect} \tag{5a}$$

$$t_{n,\,end}^{collect}=(n-1)\cdot(\Delta_{feed}+\Delta_{gap})+t_{1,\,end}^{collect} \tag{5b}$$

where $t_{1,\,start}^{collect}$ and $t_{1,\,end}^{collect}$ are the starting time and the ending time of the 1st product collection respectively.

One of the prevalent criteria in evaluating the performance of the above-explained batch chromatographic process is the productivity, which is defined here as the amount of valine product collected per unit time per unit bed volume (BV) as follows.

$$\text{Productivity}=\frac{C_A^{feed}\cdot Q\cdot\Delta_{feed}\cdot \text{Yield}_A}{BV\cdot(\Delta_{feed}+\Delta_{gap})}=\frac{C_A^{feed}\cdot Q\cdot \text{Yield}_A}{BV\cdot(1+\Delta_{gap}/\Delta_{feed})} \tag{6}$$

where the subscript A indicates valine; C_A^{feed} is the concentration of valine in the feed; Q is the volumetric flow rate; and Yield_A is the yield of valine product. The above expression shows that the productivity is controlled by the ratio of gap size to feed size ($\Delta_{gap}/\Delta_{feed}$), flow rate (Q), and product yield for a given feed concentration.

To obtain another useful expression for the productivity, one can utilize the following relationships.

$$C_A^{feed}\cdot\Delta_{feed}\cdot\text{Yield}_A=C_A^{prod}\cdot\Delta_{collect} \tag{7a}$$

$$\Delta_{collect}+\Delta_{discard}=\Delta_{feed}+\Delta_{gap} \tag{7b}$$

where C_A^{prod} is the concentration of valine in the collected product stream, and $\Delta_{collect}$ and $\Delta_{discard}$ are the lengths of product collection and waste discard in time unit, respectively, i.e., $\Delta_{collect}=t_{n,\,end}^{collect}-t_{n,\,start}^{collect}$ and $\Delta_{discard}=t_{n+1,\,start}^{collect}-t_{n,\,end}^{collect}$. Between the two above equations, the first one comes from mass balance, while the second one results from the combination of Eqs. (5a) and (5b). Using these two equations, one can transform the previous expression for the productivity (Eq. (6)) into the following.

$$\text{Productivity}=\frac{C_A^{prod}\cdot Q\cdot\Delta_{collect}}{BV\cdot(\Delta_{collect}+\Delta_{discard})}=\frac{C_A^{prod}\cdot Q}{BV\cdot(1+\Delta_{discard}/\Delta_{collect})} \tag{8}$$

This expression suggests that the productivity is governed by the ratio of discard length to collection length ($\Delta_{discard}/\Delta_{collect}$) and the product of C_A^{prod} and Q. Here, the latter term ($C_A^{prod}\cdot Q$) can be interpreted as the average mass flow rate of valine during the period of product collection.

All the key operating parameters mentioned above will be optimized in the following section in such a way that the productivity of the batch chromatographic process for separation of valine from isoleucine and leucine can be maximized under a given constraint on valine purity.

RESULTS AND DISCUSSION

1. Optimization of the Batch Chromatographic Process for Valine Separation

1-1. Definition of the Optimization Task to be Performed

One of the essential prerequisites for optimizing the batch chromatographic process under consideration is to secure the intrinsic parameters of the feed components (valine, isoleucine, and leucine) on the Amberchrom-CG161C adsorbent. These intrinsic parameters include the adsorption isotherm and mass-transfer parameters of each component, which will serve as key input data

Table 1. Intrinsic parameters and column properties used in the optimization of the batch chromatographic process for separation of valine from isoleucine and leucine [5,6]

	Valine	Isoleucine	Leucine
Henry constant (H)	0.926	4.361	5.527
Molecular diffusivity (D_∞), cm^2/min	5.10×10^{-4}	4.35×10^{-4}	5.40×10^{-4}
Intra-particle diffusivity (D_p), cm^2/min	3.00×10^{-4}	3.00×10^{-4}	5.40×10^{-5}
Axial dispersion coefficient (E_b), cm^2/min	Chung and Wen correlation [17]		
Film mass-transfer coefficient (k_f), cm/min	Wilson and Geankoplis correlation [18]		
Adsorbent particle diameter (d_p), μm	120		
Bed voidage (ε_b)	0.391		
Particle porosity (ε_p)	0.737		

in the stage of optimizing the batch chromatographic process of interest. As for the intrinsic parameters of valine, isoleucine, and leucine on the Amberchrom-CG161C adsorbent, the relevant information was reported in our recent publications [5,6]. The reported parameter values of each component are listed in Table 1.

Using the intrinsic parameters in Table 1, the batch chromatographic process of interest was optimized in this section. This task was carried out in such a way that the desired separation of valine from isoleucine and leucine could be fulfilled while maximizing productivity (Eq. (6)). For this task, the productivity (*Prod*) of the batch chromatographic process was employed as an objective function to be maximized while taking into account the following two constraints. First, the purity of valine in the collected product stream should be higher than 95%. Secondly, the pressure drop through the chromatographic bed must not exceed 100 psi, which is a general criterion for a low-pressure chromatographic separation process. The other details in such an optimization task are presented below.

Max	$J=\text{Prod}\,[\Delta_{feed}, \Delta_{gap}, t_{1,\,start}^{collect}, t_{1,\,end}^{collect}]$	(9a)
Subject to	Purity of valine≥95%	(9b)
	ΔP≤100 psi	(9c)
Dependent variables	$t_n^{feed}, t_{n,\,start}^{collect}, t_{n,\,end}^{collect}$	(9d)
Fixed variables	L_c=100 cm, d_c=2.5 cm	(9e)
	C_{feed}=5 g/L for each amino acid	(9f)

where ΔP is the pressure drop; and L_c and d_c are the length and diameter of the chromatographic bed, respectively. The three dependent variables in Eq. (9d) are related to the decision variables (or the variables to be optimized) by Eqs. (4) and (5).

To reduce the computation time for the above optimization task, the flow rate was not directly included as the variables to be optimized, as can be seen in Eq. (9a). Instead, the flow rate was changed in a discrete manner and for each step the four decision variables (Δ_{feed}, Δ_{gap}, $t_{1,\,start}^{collect}$, $t_{1,\,end}^{collect}$) were optimized. This approach can be of advantage to the analysis of the optimization results, because the effect of the flow rate on productivity can be demonstrated while finding the optimal flow rate.

To solve the optimization problem, a highly efficient genetic algorithm, NSGA-II-JG [7,8], was employed in this study. The corresponding computer-program codes for the NSGA-II-JG were prepared using Visual Basic Application (VBA) in Excel software. Since the NSGA-II-JG optimization requires repetitive numerical simulations, the VBA codes were prepared to include the function of calling Aspen Chromatography as well as of implementing the NSGA-II-JG algorithm.

1-2. Analysis of the Optimization Results for the Batch Chromatographic Process of Interest

Using the electronic tool prepared above, the optimization for the batch chromatographic process of interest was performed in accordance with the mathematical frame of Eq. (9) while varying the flow rate at the intervals of 20 mL/min. The results are presented in Fig. 3(a), where the productivity of the optimized batch process at each flow rate was plotted as a function of the flow rate.

Clearly, the productivity is largely affected by the flow rate. If the flow rate is relatively low (<140 mL/min), the productivity becomes higher as the flow rate increases. By contrast, if the flow rate is relatively high (>140 mL/min), the productivity decreases with increasing the flow rate. As a consequence, a maximum in the productivity occurs at the flow rate of 140 mL/min (u_0=72.94 cm/min), which virtually corresponds to the optimal flow rate for the batch chromatographic process of interest (point b in Fig. 3(a) and Table 2).

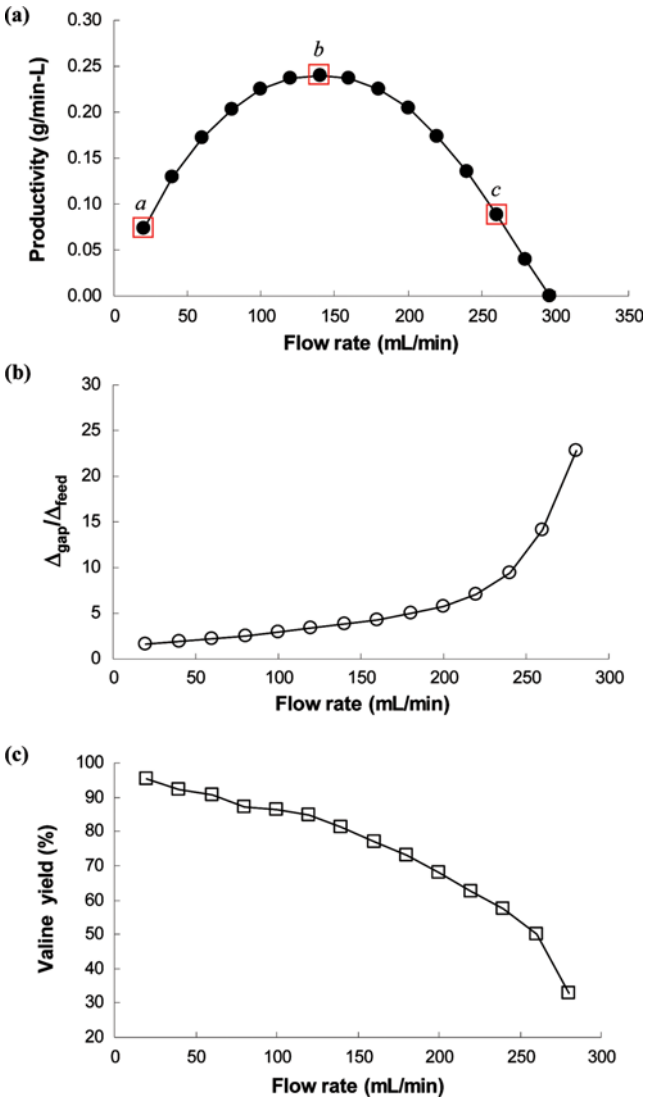

Fig. 3. Effect of the flow rate on the optimization results for the batch chromatographic process with no constraint on valine yield. (a) Productivity, (b) $\Delta_{gap}/\Delta_{feed}$, (c) valine yield.

The aforementioned phenomenon occurs because the flow rate has a considerable effect on $\Delta_{gap}/\Delta_{feed}$ and valine yield, both of which are as important as the flow rate in determining the magnitude of productivity (Eq. (6)). To examine this point in more detail, the $\Delta_{gap}/\Delta_{feed}$ value of the optimized process at each flow rate was calculated. The calculated $\Delta_{gap}/\Delta_{feed}$ values were then presented as a function of flow rate in Fig. 3(b). Note that in the region of low flow rates, the $\Delta_{gap}/\Delta_{feed}$ value increases slowly with increasing the flow rate. By contrast, in the region of high flow rates, the $\Delta_{gap}/\Delta_{feed}$ value increases sharply with increasing the flow rate. It is thus evident that the impact of the $\Delta_{gap}/\Delta_{feed}$ factor on the productivity is more pronounced in the region of high flow rates. In other words,

Table 2. The productivity and the operating parameters of the three selected processes that were marked as a, b, and c in Fig. 3(a)

	Point a	Point b	Point c
Productivity (g/min-L)	0.073	0.240	0.088
Q (mL/min)	20	140	260
u_o (cm/min)	10.42	72.94	135.46
Δ_{feed} (min)	12.902	1.400	0.323
Δ_{gap} (min)	21.455	5.360	4.562
$t^{collect}_{1,\,start}$ (min)	23.709	3.137	1.725
$t^{collect}_{1,\,end}$ (min)	36.881	4.624	2.047
t^{feed}_{n} (min)	(n−1)×34.357	(n−1)×6.760	(n−1)×4.885
$t^{collect}_{n,\,start}$ (min)	(n−1)×34.357+23.709	(n−1)×6.760+3.137	(n−1)×4.885+1.725
$t^{collect}_{n,\,end}$ (min)	(n−1)×34.357+36.881	(n−1)×6.760+4.624	(n−1)×4.885+2.047
$\Delta_{collect}$ (min)	13.172	1.487	0.322
$\Delta_{discard}$ (min)	21.185	5.273	4.563

the productivity is governed by the flow rate in the region of low flow rates, whereas it is virtually governed by the $\Delta_{gap}/\Delta_{feed}$ factor in the region of high flow rates. Besides the $\Delta_{gap}/\Delta_{feed}$ factor, it is also worth paying attention to the valine yield in Fig. 3(c). We see that the valine yield decreases with increasing the flow rate, which seems to be more significant in the region of high flow rates (Fig. 3(c)). Due to such effect of the flow rate on the valine yield and the $\Delta_{gap}/\Delta_{feed}$ factor, the productivity increases and then decreases with increasing the flow rate as seen in Fig. 3(a).

The occurrence of the aforementioned trends of $\Delta_{gap}/\Delta_{feed}$ and valine yield is mostly attributed to the relationship between column efficiency (or mass-transfer efficiency) and liquid linear velocity (or flow rate for a fixed column diameter). In general, as the linear velocity increases, the column efficiency becomes lower and the mass-transfer resistance becomes more severe, which makes each solute band more spread. For such reason, the increase of liquid linear velocity causes the following two undesirable cases in regard to the separation task of our interest: (1) the possible contamination of valine (product) by the leucine (impurity) band of the preceding feed batch, and (2) the possible contamination of valine (product) by the isoleucine and leucine (impurities) bands of the same feed batch. To protect the valine purity (≥95%) against such two undesirable cases, the gap size must be enlarged and the collected amount of valine must be reduced, if needed. This is why an increase in the flow rate leads to a higher $\Delta_{gap}/\Delta_{feed}$ value and a lower valine yield, as seen in Figs. 3(b) and 3(c).

1-3. Comparison of the Effluent Histories of the Batch Chromatographic Processes Optimized at Different Flow Rates

In the previous section, the batch chromatographic process of interest was optimized while varying the flow rate discretely. It would be worthwhile to compare the effluent histories of such processes. For this task, the simulations were performed for the three selected processes in Fig. 3(a) (points a, b, and c), one of which was based on the optimal flow rate (140 mL/min) and the other two were based on the lower and the higher flow rates than the optimal one, respectively (20 mL/min and 260 mL/min). The detailed operating parameters for these three processes are listed in Table 2. The effluent histories resulting from the simulations for such processes are presented in Fig. 4, where the mass flow rate of each component exiting the column outlet was plotted with respect to the exit time. Here, the mass flow rate was obtained by multiplying the effluent concentration (C_{out}) by the flow rate (Q).

Note first that the effluent from the process based on the lowest flow rate (Fig. 4(a)) has a significantly lower mass flow rate, compared to those based on the other flow rates (Figs. 4(b) and 4(c)). Also, the process based on the highest flow rate (Fig. 4(b)) has a significantly higher $\Delta_{discard}/\Delta_{collect}$, compared to those based on the other two flow rates (Figs. 4(a) and 4(c)). Obviously, such a significantly low mass flow rate or a significantly high $\Delta_{discard}/\Delta_{collect}$ will have an adverse effect on the productivity, which can easily be understood from Eq. (8).

By contrast, the effluent history for the process based on the optimal flow rate (Fig. 4(c)) reveals that the aforementioned two factors (mass flow rate and $\Delta_{discard}/\Delta_{collect}$) are well balanced, which will surely be effective in attaining high productivity.

2. Optimization of the Batch Chromatographic Process for Valine Separation under the Yield Constraint

The yield of a product component can sometimes be as important as process productivity, particularly when the product is a highly valuable one. In this case, the issue of placing a constraint on product yield needs to be considered for the purpose of maintaining the yield higher than its target level during the process optimization. To investigate such issue for the batch chromatographic process of our interest, additional optimization was performed under the constraint of valine yield ≥80% while all the other conditions were kept the same as in the previous section. This task was then repeated by varying only the target level in the yield constraint from 80% to 90% and 95%. The results from such a series of optimizations are presented in Fig. 5(a), where the results from the previous optimizations under no constraint on valine yield were added for comparison purpose.

Note in Fig. 5(a) that the productivity decreases with tightening the yield constraint, which trend is pronounced mostly in the region of the flow rates higher than the optimal one. The occurrence of such phenomenon is closely related to the fact that the use of a larger eluent gap between two adjacent feed batch injections is essential for increasing the region of the purified valine band, and thus meeting the tightened yield requirement, even if it can reduce

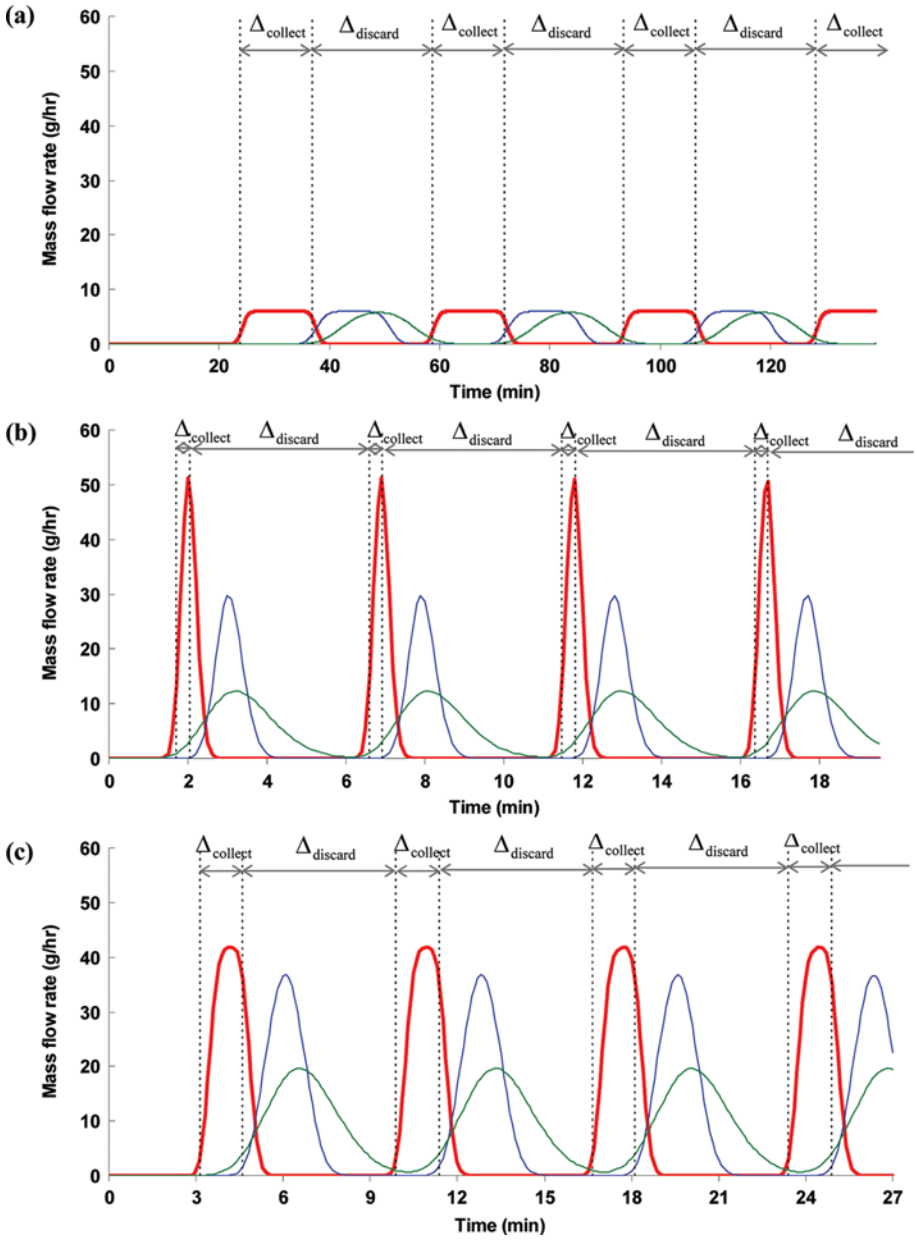

Fig. 4. Effluent histories of the batch chromatographic processes that were optimized at three different flow rates under no constraint on valine yield. (a) Q=20 mL/min, (b) Q=260 mL/min, (c) Q=140 mL/min (optimal flow rate). The operating conditions of these three processes are listed in Table 2.

the productivity as a result of the severely increased gap size. To check this point in detail, the $\Delta_{gap}/\Delta_{feed}$ values of all the optimized processes under the yield constraints considered were calculated and the results were compared in Fig. 5(b).

It is readily seen that in the region of high flow rates, the $\Delta_{gap}/\Delta_{feed}$ value is significantly increased as the target level of the valine yield is set higher. In such case, the adverse effect of the increased $\Delta_{gap}/\Delta_{feed}$ value on the productivity can outweigh the positive effect of the increased yield on the productivity. For this reason, the productivity of the optimized process in the region of high flow rates undergoes a sharp reduction with tightening the yield constraint (Fig. 5(a)).

By contrast, in the region of low flow rates, the $\Delta_{gap}/\Delta_{feed}$ value is observed to be little affected by the target level in the yield constraint (Fig. 5(b)). The major reason for such phenomenon is that if the flow rate is lower (i.e., the column efficiency is higher), the optimum of the process tends to occur at higher yield, regardless of the given yield constraint. In such case, the yields of the optimized processes can be high enough to exceed the target levels in the yield constraints. For this reason, the optimized processes under different yield constraints become equal or similar in productivity as well as in yield, if the flow rate is sufficiently low to ensure high column efficiency (Fig. 5(a)).

In addition to the above analysis, the optimized processes under

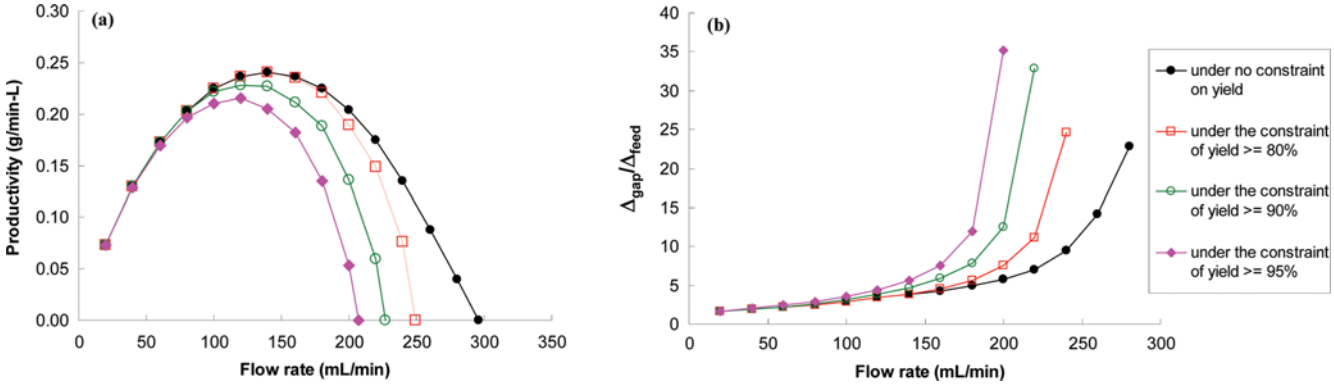

Fig. 5. Effect of the target level of the yield constraint on the optimization results for the batch chromatographic process. (a) Productivity, (b) $\Delta_{gap}/\Delta_{feed}$.

different yield constraints in Fig. 5(a) are also worthy to be compared in terms of their maximum productivities occurring at the corresponding optimal flow rates. For this task, the maximum productivities that are attainable under all the yield constraints considered are listed in Table 3. As expected, the maximum productivity is reduced as the yield constraint is tightened. However, it is worth noting that the maximum productivity of the optimized process under the most tightened yield constraint (≥95%) in Table 3 is only 10% lower than that under no yield constraint (point b in Table 2). In such case, the selection of the batch separation process leading

Table 3. The maximum productivities and the optimal operating parameters of the batch chromatographic processes that were optimized under different constraints of valine yield

	Valine yield≥80%	Valine yield≥90%	Valine yield≥95%
Productivity (g/min-L)	0.240	0.228	0.215
Q (mL/min)	140	120	120
u_o (cm/min)	72.94	62.52	62.52
Δ_{feed} (min)	1.400	1.480	1.359
Δ_{gap} (min)	5.360	5.675	5.977
$t^{collect}_{1,\,start}$ (min)	3.137	3.673	3.609
$t^{collect}_{1,\,end}$ (min)	4.624	5.453	5.491
t^{feed}_{n} (min)	(n−1)×6.760	(n−1)×7.155	(n−1)×7.336
$t^{collect}_{n,\,start}$ (min)	(n−1)×6.760+3.137	(n−1)×7.155+3.673	(n−1)×7.336+3.609
$t^{collect}_{n,\,end}$ (min)	(n−1)×6.760+4.624	(n−1)×7.155+5.453	(n−1)×7.336+5.491
$\Delta_{collect}$ (min)	1.487	1.780	1.882
$\Delta_{discard}$ (min)	5.273	5.375	5.454

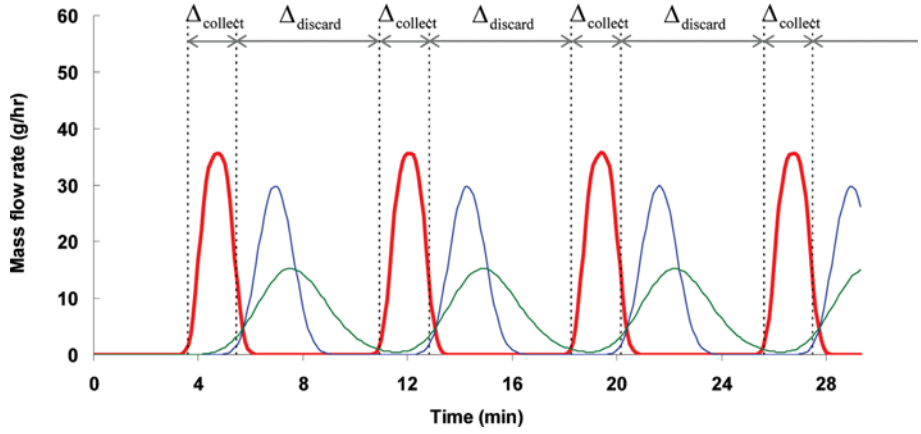

Fig. 6. Effluent history of the optimal batch chromatographic process leading to the maximum productivity under the constraint of yield ≥95%. The operating conditions of this process are listed in Table 3.

to higher valine yield at the expense of some productivity can sometimes be of benefit to the process economics, because the valine product has many valuable applications in industry.

The effluent histories for the two aforementioned processes are presented in Figs. 4(c) and 6, which can be compared in terms of the collected portion and the mass flow rate that are closely related to the yield and the productivity respectively. We see that the optimized process under the yield constraint (≥95%) collects a larger portion of valine in each relevant solute band while having a little reduction in the mass flow rate, compared to the optimized process under no yield constraint. This leads the former process to make a meaningful improvement in the valine yield while making the extent of the productivity reduction as low as possible.

CONCLUSIONS

A batch chromatographic process customized for separation of valine from isoleucine and leucine was optimally designed. This work involved using an optimization tool for the batch chromatographic process, which was prepared on the basis of a highly efficient genetic algorithm: NSGA-II-JG. This optimization task was carried out in such a way that the valine productivity of the batch chromatographic process could be maximized under a given purity requirement. The results showed that the valine productivity was governed by the flow rate in the region of low flow rates, whereas it was governed by the $\Delta_{gap}/\Delta_{feed}$ factor in the region of high flow rates. As a consequence, the optimum of the process occurred when the liquid linear velocity and the $\Delta_{gap}/\Delta_{feed}$ value were 72.94 cm/min and 3.83, respectively. Also, the valine productivity of the optimized process was reduced as the target level in the constraint for valine yield was set higher. The amount of such productivity reduction, however, was not so large. If the target level in the yield constraint was 95%, the optimum of the process, which occurred at the liquid linear velocity of 62.52 cm/min, had only 10% reduction, compared to that under no yield constraint. All of the results in this study will contribute to a substantial improvement in the economic efficiency of the valine production process.

ACKNOWLEDGEMENTS

This research was supported by Basic Science Research Program through the National Research Foundation of Korea (NRF) funded by the Ministry of Science, ICT and Future Planning (grant number NRF-2015R1A2A2A01003455). Also, it was partially supported by the Advanced Biomass R&D Center (ABC) of Global Frontier Project funded by the Ministry of Science, ICT and Future Planning (ABC-2010-0029728).

REFERENCES

1. T. Hermann, *J. Biotechnol.*, **104**, 155 (2003).
2. B. Blombach, M. E. Schreiner, J. Holatko, T. Bartek, M. Oldiges and B. J. Eikmanns, *Appl. Environ. Microbiol.*, **73**, 2079 (2007).
3. J. H. Park, K. H. Lee, T. Y. Kim and S. Y. Lee, *Proc. Natl. Acad. Sci. U.S.A.*, **104**, 7797 (2007).
4. M. Wada, N. Hijikata, R. Aoki, N. Takesue and A. Yokota, *Biosci. Biotehnol. Biochem.*, **72**, 2959 (2008).
5. C. Park, H. G. Nam, H. J. Hwang, J. H. Kim and S. Mun, *Process Biochem.*, **49**, 324 (2014).
6. C. H. Lee, S. H. Kang, J. H. Yoo, Y. S. Kim, S. Mun, H. G. Nam and C. Park, KR Patent, 10-1449808 (2014).
7. R. B. Kasat and S. K. Gupta, *Comput. Chem. Eng.*, **27**, 1785 (2003).
8. K. B. Lee, R. B. Kasat, G. B. Cox and N. H. L. Wang, *AIChE J.*, **54**, 2852 (2008).
9. M. A. Cremasco, B. J. Hritzko, Y. Xie and N. H. L. Wang, *Braz. J. Chem. Eng.*, **18**, 181 (2001).
10. Z. Ma and N. H. L. Wang, *AIChE J.*, **43**, 2488 (1997).
11. B. J. Hritzko, Y. Xie, R. Wooley and N. H. L. Wang, *AIChE J.*, **48**, 2769 (2002).
12. Y. Xie, B. Hritzko, C. Y. Chin and N. H. L. Wang, *Ind. Eng. Chem. Res.*, **42**, 4055 (2003).
13. K. B. Lee, C. Y. Chin, Y. Xie, G. B. Cox and N. H. L. Wang, *Ind. Eng. Chem. Res.*, **44**, 3249 (2005).
14. S. H. Kang, S. I. Jeon, K. H. Lee, J. H. Kim and S. Mun, *J. Liq. Chromatogr. Rel. Technol.*, **31**, 2053 (2008).
15. H. G. Nam, S. H. Jo and S. Mun, *Process Biochem.*, **46**, 2044 (2011).
16. Q. Han, C. G. Yoo, S. H. Jo and S. Mun, *J. Chem. Eng. Data*, **53**, 2613 (2008).
17. S. F. Chung and C. Y. Wen, *AIChE J.*, **14**, 857 (1968).
18. E. J. Wilson and C. J. Geankoplis, *Ind. Eng. Chem. Fundam.*, **5**, 9 (1966).
19. C. R. Wilke and P. I. N. Chang, *AIChE J.*, **1**, 264 (1955).
20. J. S. Mackie and P. Meares, *Proc. Roy. Soc. London Ser. A*, **232**, 498 (1955).